Preparation and Characterization of Poly(butadiene-*stat*-styrene)/Poly(styrene-*stat*-acrylonitrile) Structured Latex Particles

R. HU,[1,2] V. L. DIMONIE,[1] M. S. EL-AASSER[1,3]

[1] Emulsion Polymers Institute, [2] Department of Chemistry, and [3] Department of Chemical Engineering, Lehigh University, Bethlehem, Pennsylvania 18015

Received 26 June 1996; accepted 10 October 1996

ABSTRACT: In rubber toughening of thermoplastics, core/shell polymers have been used extensively. This work introduces the synthesis and characterization of polybutadiene based core/shell latex particles with controlled particle size and crosslinking density of the core. A lithium soap recipe was employed to prepare a series of poly(butadiene-*stat*-styrene) (90/10 by wt) core particles by conventional emulsion polymerization through a batch process. The shell polymer, poly(styrene-*stat*-acrylonitrile) (72/28 by wt), was polymerized by a semicontinuous process in the presence of the core particles to form a core/shell morphology. The effects of initiator concentration, monomer feeding rate, core/shell ratio, and gel-fraction of the core on the core/shell particle morphology were studied. The degree of grafting of the shell polymer on the core particles was determined as well. The morphology and glass transitions of these particles were characterized by transmission electron microscopy, differential scanning calorimetry, and dynamic mechanical spectroscopy. These latex particles can be used specifically in toughening polycarbonate. © 1997 John Wiley & Sons, Inc. J Appl Polym Sci **64:** 1123–1134, 1997

INTRODUCTION

In the art of toughening thermoplastics for impact resistance, the utilization of the class of rubbery core/glassy shell polymers is well known, due to three major attractive features: 1) the rubbery core provides resistance to impact, especially at low temperatures, whereas the grafted glassy shell provides rigidity and compatibility to the polymer matrix, keeping the particle's desired shape and dispersibility; 2) the rubber particle size, particle size distribution, crosslink density, degree of grafting of the shell polymer on the core polymer, shell thickness, and shell composition on the toughening property and mechanisms, as well as overall composition, can be individually studied and optimized; and 3) the versatility of emulsion polymerization provides a convenient control on the synthesis of the desired particles as outlined above.[1–8] Core/shell polymers are commercially available for the above applications.

There are basically two typical types of rubbery cores, polybutadiene (PBd) and acrylic-based polymers, both of which can be synthesized through emulsion polymerization and be used as toughening modifiers.[9–13] Since PBd is an excellent rubber even at very low temperatures (T_g = −85°C) and is cheaper than the acrylic polymers, PBd is the elastomer of choice as the rubber toughening agent for many practical applications.

Correspondence to: Mohamed El-Aasser.
Present Address: Dept. of Chemical Engineering, Lehigh University, 111 Research Drive, Iacocca Hall, Bethlehem, PA 18015-4732.

On the other hand, the shell polymer is selected based on the good compatibility between the shell and the polymer matrix to achieve a certain dispersibility and good adhesion with the matrix.

In spite of a large amount of literature published on the fracture behavior of polycarbonates (PC), only a few studies have dealt with rubber-modified PC.[14–17] Cheng et al. studied the toughening properties of PC modified with three kinds of elastomeric modifiers: linear polybutadiene (PBd), linear styrene-butadiene-styrene block copolymer (SBS), and PBd core/poly(methyl methacrylate-*co*-styrene) shell polymer (MBS).[17] They found that the best impact was achieved with PC/MBS blends, good impact was obtained with PC/SBS blends when SBS was dispersed as aggregates of small particles, and PBd did not significantly enhance the impact strength of PC. Lombardo, Keskkula, and Paul investigated the influence of ABS type on morphology and mechanical properties of PC/ABS blends.[18] Bulk ABS and emulsion ABS with different rubber contents varying from 16% to 50% were used in blends with PC to make comparisons at constant rubber concentrations of 5, 10, and 15%. It was concluded that small rubber particles can toughen PC/ABS blends at lower rubber concentrations and at lower temperatures. Recently, Segall et al. investigated the rubber toughened PC using poly(*n*-butyl acrylate) (PBA)/poly(benzyl methacrylate-styrene) structured latex particles.[19–21] The effect of particle size and levels of crosslinking of the rubbery core, composition, and molecular weight of the shell polymer, the weight ratio of shell to core polymers, and the particle morphologies on toughening PC were systematically studied. It has been found that the toughness of polycarbonates was improved when using core/shell particles with thinner shells (3–18 nm); at lower temperature, using large rubber particles (350 nm in diameter) instead of small particles (173 nm in diameter) the improvement of impact resistance was more effective. The crosslinking density of the poly(butyl acrylate) rubbery core has little effect on the toughening properties.

In this work, further study was done on a modified PC system using core/shell type latex particles with poly(butadiene-*stat*-styrene) [P(Bd/S)] as the rubbery cores and poly(styrene-*stat*-acrylonitrile) (SAN), which possesses a high grafting efficiency onto the P(Bd/S) core and is compatible with PC,[22–24] as the shell. The size and crosslinking density of the rubbery particle, thickness and composition of the shell polymer, and degree of grafting of the shell polymer on the core polymer were controlled to study the effect of these factors on toughening properties. In a separate paper,[25] the mechanical and toughening properties of PC modified by these latex particles will be presented.

EXPERIMENTAL

Materials

Butadiene (Bd) (Matheson Gas Products, Inc.) and styrene (S) (Aldrich) were purified by passing them through the Ascarite II (Thomas Scientific) and the aluminum oxide (Aldrich) columns, respectively. Acrylonitrile (AN) was distilled before use. Potassium persulfate ($K_2S_2O_8$, or KPS) was used as an initiator without further purification. Dodecyl mercaptan (DDM) was used as a chain transfer agent, without further purification. Lithium hydroxide (LiOH), lithium carbonate (Li_2CO_3), stearic acid (SA), lithium stearate, and Dowfax 2A1 (sodium disulfonated dodecyl alkylated diphenyl oxide, Dow Chemical Co.) were used as received. The water used in all synthesis process was distilled deionized water (DDI).

Synthesis of P(Bd/S) Cores with Different Particle Sizes and Gel Fractions

Since previous research[26] has shown that monodisperse P(Bd/S) (40/60 by wt) latex particles up to 560 nm could be prepared using lithium soap recipes through emulsion polymerization by a batch process, monodisperse P(Bd/S) (90/10 by wt) latex particles with high and medium gel fractions were prepared for this study from the recipes shown in Table I using a pressurized bottle emulsion polymerization process. The aqueous phase (DDI water, LiOH, Li_2CO_3, and KPS) was added in the bottle first, and mixed with the oil phase (S, DDM, and SA) to form an emulsion. The polymerization was carried out at 70°C by end-over-end rotation at 32 rpm. SA reacted with LiOH *in situ* to form the surfactant, lithium stearate. Li_2CO_3 was added to control (retard) the solubility of lithium stearate because of the common ion effect, and hence the particle size. A series of monodisperse P(Bd/S) (90/10 by wt) latex particles were synthesized as well by varying the SA, LiOH, and Li_2CO_3 concentrations. Preformed lithium stearate salt was also used as an emulsifier instead of the *in situ*-formed lithium stearate

Table I Recipes for Preparation of P(Bd/S) Cores with Different Gel Fractions (70°C, 24 h, 32 rpm)

Component	High Gel Recipe Parts, g	Medium Gel Recipe Parts, g
Distilled-deionized water (DDI)	180	180
Bd/S (90/10 by wt)	100	100
Potassium persulfate (KPS)	0.50	0.4
Dodecyl mercaptan (DDM)	0.10	0.1
Stearic acid (SA)	1.84	0.69
Lithium hydroxide (LiOH)	0.156	0.059
Lithium carbonate (Li_2CO_3)	—	0.056

from SA and LiOH to see the effect on particle size.

Synthesis of P(Bd/S)/SAN-Structured Latex Particles

The structured P(Bd/S) core/SAN shell latex particles were prepared by the semicontinuous emulsion polymerization process. The core was P(Bd/S) (90/10 by wt) latex particles with 95% gel-fraction, otherwise specified. The shell polymer was selected to be SAN (S/AN 72/28 by wt). The core/shell ratio was varied to control the thickness of the shell. KPS (0.06% on total) was used as the initiator, and same amount of $NaHCO_3$ was used as a buffer. An additional emulsifier, Dowfax 2A1 (0.06% on total), was added in order to obtain a stable latex without forming secondary particles. A preemulsion was made from the styrene-acrylonitrile monomer mixture and Dowfax 2A1 emulsifier. The KPS initiator was charged initially into the reactor and allowed to react to form seed particles *in situ*. Ten percent of the preemulsion was charged into the core latex first. After 0.5 h, the remaining preemulsion was continuously fed under monomer-starved conditions.

Characterization

Three techniques, dynamic light scattering (Nicomp), capillary hydrodynamic fractionation (CHDF), and transmission electron microscopy (TEM, Philips 300), were used to measure the average latex particle size and particle size distribution. The polydispersity index (PDI) was given as the ratio of the weight-to-number average diameters, D_w/D_n. For TEM measurement, the core particles were positively stained with osmium tetroxide (OsO_4) and at least 500 particles for each sample were measured from the micrographs using a Zeiss MOP-3 analyzer. The morphologies of core/shell particles were also studied by TEM (Philips EM400T), with the particles stained both positively with OsO_4 for the core and negatively with phosphotungstic acid (PTA) for the background.

The gel fraction of the P(Bd/S) core particles was determined by a solvent extraction method. The latex particles were first dried at room temperature. Then, 0.2 g of the polymer film was swollen by 25 g toluene for 48 h, followed by centrifugation for 1 h at 3000 rpm. Then, 2.5 g of the supernatant containing the soluble P(Bd/S) was dried in an oven at 75°C until a constant mass is achieved. The gel fraction (G.F.) was determined as follows:

$$\text{G.F.}(\%) = \frac{0.2 - w}{0.2} \times 100 \qquad (1)$$

where w is the total mass of the dried soluble P(Bd/S) in the supernatant.

The crosslinking density of latex particles was determined based on the equilibrium swelling theory of Flory and Rehner. The Flory-Rehner equation (eq. 2) is used to calculate the number of elastically active chains per unit volume, n (see Table III).[27]

$$-[\ln(1 - \nu_2) + \nu_2 + \chi_1\nu_2^2] = V_1 n\left[\nu_2^{1/3} - \frac{\nu_2}{2}\right] \qquad (2)$$

where ν_2 is the volume fraction of polymer in the swollen mass, V_1 is the molar volume of the solvent, and χ_1 is the Flory-Huggins polymer-solvent dimensionless interaction term. For the P(Bd/S)

latex particles in this work, toluene was used as the solvent. The dried latex film was cut in rectangular shape. The film dimension was measured and put in excess toluene for 24 h at room temperature. Then the dimension of the film was measured again. For the system P(Bd/S) and toluene, χ_1 is 0.39, and the quantity of V_1 is 106.3 cm^3/mol for toluene.[27]

The glass transition temperatures (T_g) were measured by differential scanning calorimetry (DSC, Mettler DSC30) on 20 mg samples. The heating rate was 10°C/min, from −120 to 150°C. Dynamic mechanical spectroscopy (DMS, Rheometrics RDA II) was used to determine the T_g values from the storage shear modulus, loss shear modulus, and tan δ peaks. The dried samples were compression molded at 150°C into 60 × 10 × 1 mm specimens. The temperature sweep range was −120 to 160°C. All measurements were done at 1 Hz frequency.

The grafting efficiency of the shell polymer on the core polymer was determined by a solvent extraction method. Acetone was selected as the solvent, which is a good solvent for SAN but not for P(Bd/S). The latex samples were first dried in a vacuum oven for 48 h. Then, 0.2 g of the dried sample was mixed with 10 mL acetone in a 2 oz. bottle. After mixing for 24 h at room temperature, the solution was ultracentrifuged at 30,000 rpm for 1 h at 5°C; then 5 mL of the supernatant layer was pipetted into a preweighed aluminum pan and dried, first at room temperature and then for 1 h at 75°C, to remove the acetone. The samples were cooled in a desiccator for several hours and weighed. The degree of grafting was determined by difference, similar to the gel fraction measurement.

RESULTS AND DISCUSSION

Particle Size and Crosslinking Density of P(Bd/S) Core Particles

Table II shows the particle size and polydispersity index (PDI) for the P(Bd/S) latex particles. It can be seen that the particle size increased with the decrease in SA concentration, since for a typical emulsion polymerization the particle number depends on the emulsifier concentration.[28] The higher the emulsifier concentration, the greater the number of particles, and the smaller the particle size is. In the presence of Li_2CO_3, the particle sizes of the latexes were controlled by employing lithium stearate emulsifier in the presence of lithium common ions. This control is a result of the insoluble nature of lithium stearate, which does not permit the nucleation of a larger number of particles and of the further suppression of its solubility exerted by the added lithium ions from Li_2CO_3. It is also found that the largest particle size of ~ 400 nm (TEM) was obtained when preformed lithium stearate salt was used. This is possibly because the concentration of lithium stearate formed *in situ* from SA and LiOH was higher than the preformed lithium stearate, which caused the formation of more micelles, and, consequently, smaller particle size.

It is also shown in Table II that for sample E the difference between the particle sizes measured from Nicomp and TEM is ~ 170 nm, which is possibly caused by the deformation of the P(Bd/S) particles under the electron beam. Since P(Bd/S) particles contain 90% butadiene, the beam damage is inevitable, although the particles are stained with OsO_4. Therefore, it is more correct to measure the size of the soft rubber particles in the latex form. But, on the other hand, TEM can show very clear picture in terms of the shape of the particle, size of the domains (if exists), and particle size distribution. Figure 1 is the TEM micrographs of these P(Bd/S) particles. Obviously, these particles are highly monodisperse.

By controlling the conversion and concentration of Li_2CO_3, submicron P(Bd/S) latex particles with 95 and 40% gel fractions were obtained, as shown in Table III. From the equilibrium swelling test of latex films in toluene and applying the Flory-Rehner equation (eq. 2) it was calculated n, the number of elastically active chains per unit volume. In the latex particles with a higher gel fraction (95%) the number of chains in the crosslinked network was higher and the molecular weight between crosslinks (M_c) shorter than in the low gel fraction particles (lower crosslink density). Both particles were used as the seed in a second-stage emulsion polymerization for the synthesis of structured latex particles. For P(Bd/S) particles with 40% conversion, unreacted monomers were stripped out before their use as seed in the second stage polymerization.

Morphology of P(Bd/S)/SAN Structured Latex Particles

Effect of KPS Concentration and Feeding Rate

Although a more uniform shell can be formed onto the core by the semicontinuous process for the

Table II Particle Size of Monodisperse P(Bd/S) Latex Particles

Sample	SA[a] (g)	Li_2CO_3 (g)	Lithium stearate	Nicomp (D_n, nm)	TEM (D_n, nm)	TEM PDI
A	4.1	—	—	151	135	1.02
B	1.84	—	—	235	190	1.01
C	—	—	1.88	283	250	1.01
D	0.69	0.056	—	341	320	1.00
E	—	0.037	0.93	540	375	1.00

[a] SA = stearic acid.

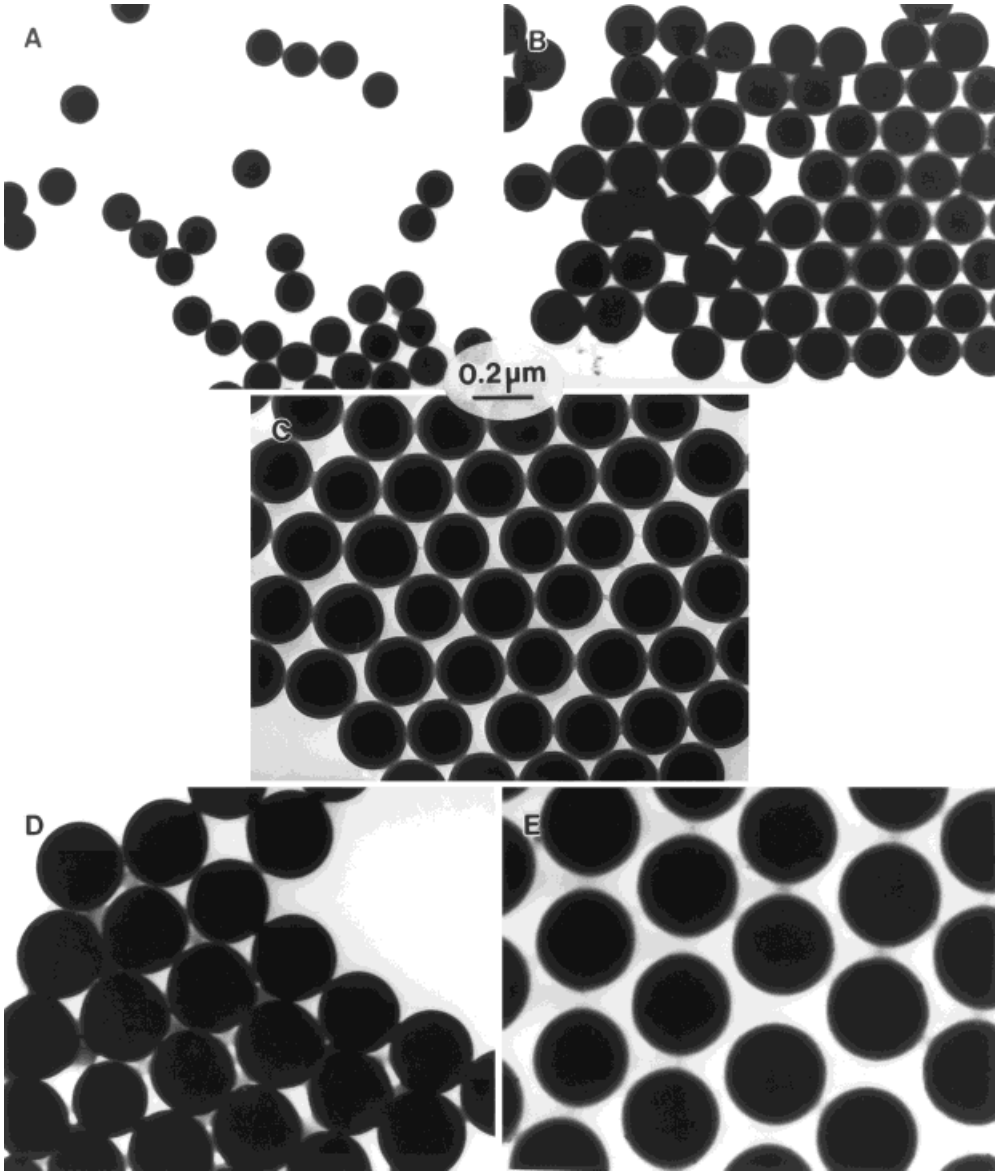

Figure 1 TEM micrographs of monodisperse P(Bd/S) latex particles: (A) 135 nm; (B) 190 nm; (C) 250 nm; (D) 320 nm; and (E) 375 nm. The particles were stained with osmium tetroxide.

Table III Physical Properties of P(Bd/S) Latex Particles with Different Crosslinking Densities

Sample		A	B
Nicomp	D_n, nm	208	259
	D_v, nm	230	281
CHDF	D_n, nm	203	270
	PDI	1.02	1.01
TEM	D_n, nm	180	230
	PDI	1.02	1.02
Conv., %		100	45
G.F., %		95	40
n, mol/cm^3		3.66×10^{-5}	1.85×10^{-6}
M_c, g/mol[a]		2.7×10^4	5.2×10^5

[a] M_c is the molecular weight between the crosslinks, which is calculated from the density of the polymer divided by n.

second stage polymerization (kinetic control), the initiator concentration and the feed rate of the second-stage monomer also could affect the final particle morphology. Figure 2 shows the effect of KPS concentration and the feeding rate of the second stage monomer on the particle morphology. These results show that for the same feed rate, the shell is smoother at higher KPS concentrations [compare Figure 2(A) and 2(B)]. Similar shell morphologies resulted when the monomer feed time was increased from 3 to 5 h, at the lower KPS concentration [compare Figure 2(A) and 2(C)]. The use of KPS in the second stage apparently results in greater anchoring of the SAN phase onto the P(Bd/S) particles by the water-soluble ionic chain end-groups. The ionic groups at the polymer chain ends rendered the SAN surface more polar, and thus the SAN phase could remain on the outside of the particle and cover the P(Bd/S) surface more uniformly. A higher KPS concentration generates more radicals, and consequently more ionic chain end-groups are formed. Thus, the SAN becomes more polar, which favors the formation of uniform shell. The feeding of the second stage monomer over a period of 3 h resulted in monomer-starved conditions, and therefore, little apparent improvement in the shell morphology was achieved by further lowering the monomer feed rate (feeding same amount of monomer over a period of 5 h). The P(Bd/S)/SAN structured latex particles were all prepared using 0.2% KPS at 5 h feeding time of the monomer.

Effect of Core/Shell (C/S) Ratio

Different polymer shell thicknesses can be attained by controlling the ratio of shell monomer to core polymer. Structured latex particles with three C/S ratios were prepared, and the particle sizes measured by Nicomp and CHDF (Table IV). The theoretical size of core/shell particles can be calculated based on the assumption that if stable core/shell particles were obtained without the formation of secondary small particles, the number for the seed particles and the core/shell particles should be the same, i.e., all the shell polymer was coated only on the existing core particles. The theoretical size for the core/shell particles was calculated from the mass balance as shown in the following equations.

$$N_{\text{core}} = \frac{W_{\text{core}}/\rho_{\text{core}}}{\frac{1}{6}\pi D_{\text{core}}^3} \tag{3}$$

$$N_{\text{core}} = N_{\text{core/shell}} \tag{4}$$

$$\frac{W_{\text{shell}}}{\rho_{\text{shell}}} = N_{\text{core/shell}} \left(\frac{1}{6}\pi D_{\text{core/shell}}^3 - \frac{1}{6}\pi D_{\text{core}}^3 \right) \tag{5}$$

$$\frac{D_{\text{core/shell}}}{D_{\text{core}}} = \sqrt[3]{1 + \left(\frac{W_{\text{shell}} + \rho_{\text{core}}}{W_{\text{core}} \times \rho_{\text{shell}}} \right)} \tag{6}$$

where N is the number of particles for the core and core/shell particles; W is the weight of the polymer; D is the particle diameter, ρ is the density of the polymer; the appropriate subscripts, core, shell, and core/shell are used.

The particle diameters of the structured latex particles for all three C/S ratios were in good agreement with the diameters predicted based on the recipe. The morphologies presented in Fig. 3 show that at these C/S ratios the core particles are all covered uniformly by the shell polymer, and the shell layer becomes thicker with an increase in the amount of the shell polymer.

Effect of Gel-Fraction of the P(Bd/S) Core

The gel-fraction of the rubber particles determines its cohesive strength, which controls the toughening mechanism due to cavitation. The effect of the gel-fraction of the core particles on the shell thickness and morphology were also studied using the P(Bd/S) cores with 40% gel-fraction as described earlier in this report. The same experimental conditions as those used for the 95% gel-fraction P(Bd/S) cores were applied, and the particle sizes at different C/S ratios were in a very good agreement with the predicted diameters (based on Nicomp measurement). However, the

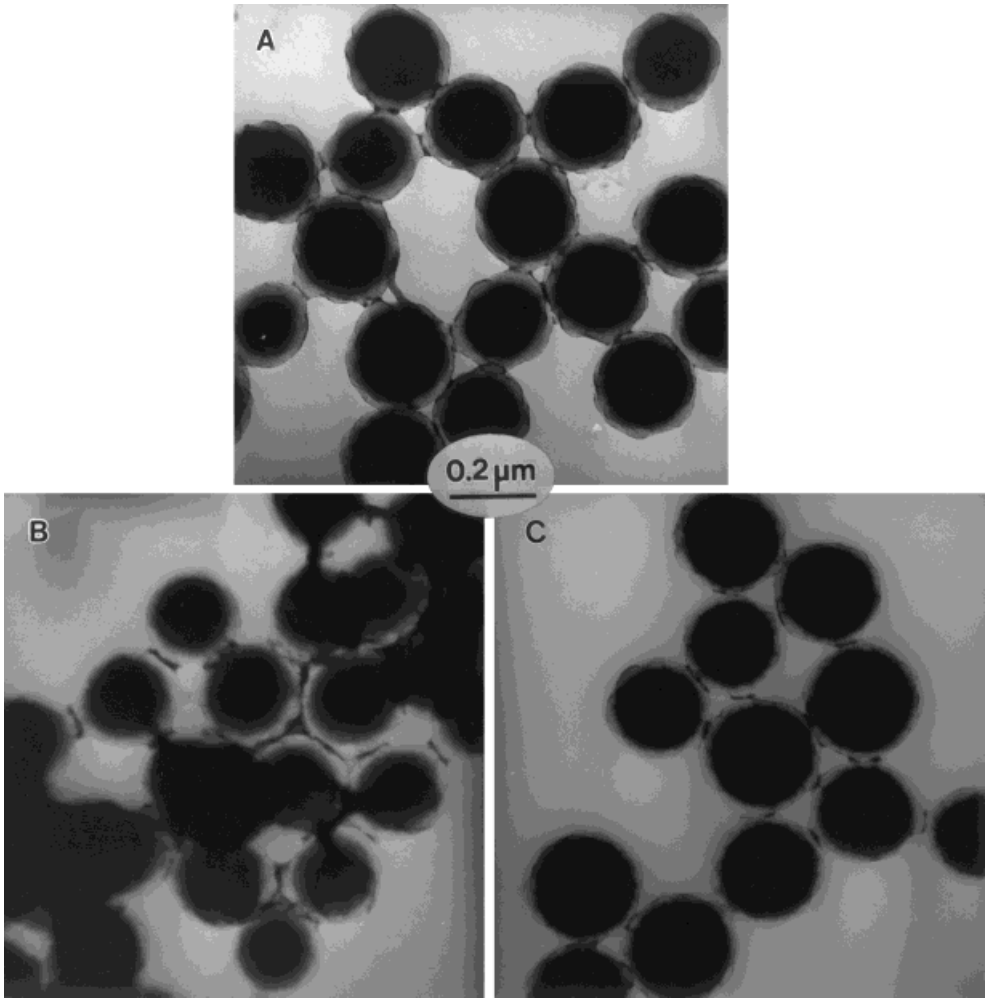

Figure 2 TEM micrographs of P(Bd/S)/SAN structured latex particles prepared by semi-continuous emulsion polymerization: (A) [KPS] = 0.06%, monomer feed over 3 h; (B) [KPS] = 0.2%, monomer feed over 3 h; (C) [KPS] = 0.06%, monomer feed over 5 h. The lighter regions are SAN, with the darker regions representing P(Bd/S). The particles were positively stained with osmium tetroxide (OsO_4) and negatively stained with phosphotungstic acid (PTA).

shell morphology, as shown in Figure 4, is not as smooth as in the cases using the P(Bd/S) cores with 95% gel-fraction. The P(Bd/S) cores with 40% gel-fraction can be swollen to a greater extent, and then they can incorporate within them more of the second-stage monomers and polymers. Upon polymerization, a phase-separated IPN-like structure probably forms within the particles.

Table IV Particle Sizes of Structured Latex Particles [P(Bd/S) cores with 95% gel-fraction]

Core/Shell wt. ratio	Theoretical D_n, nm	Nicomp D_n, nm	CHDF D_n, nm	CHDF PDI
1/0 (seed)	—	208	203	1.02
1/0.5	238	228	243	1.02
1/1	262	248	258	1.01
1/2	300	283	294	1.01

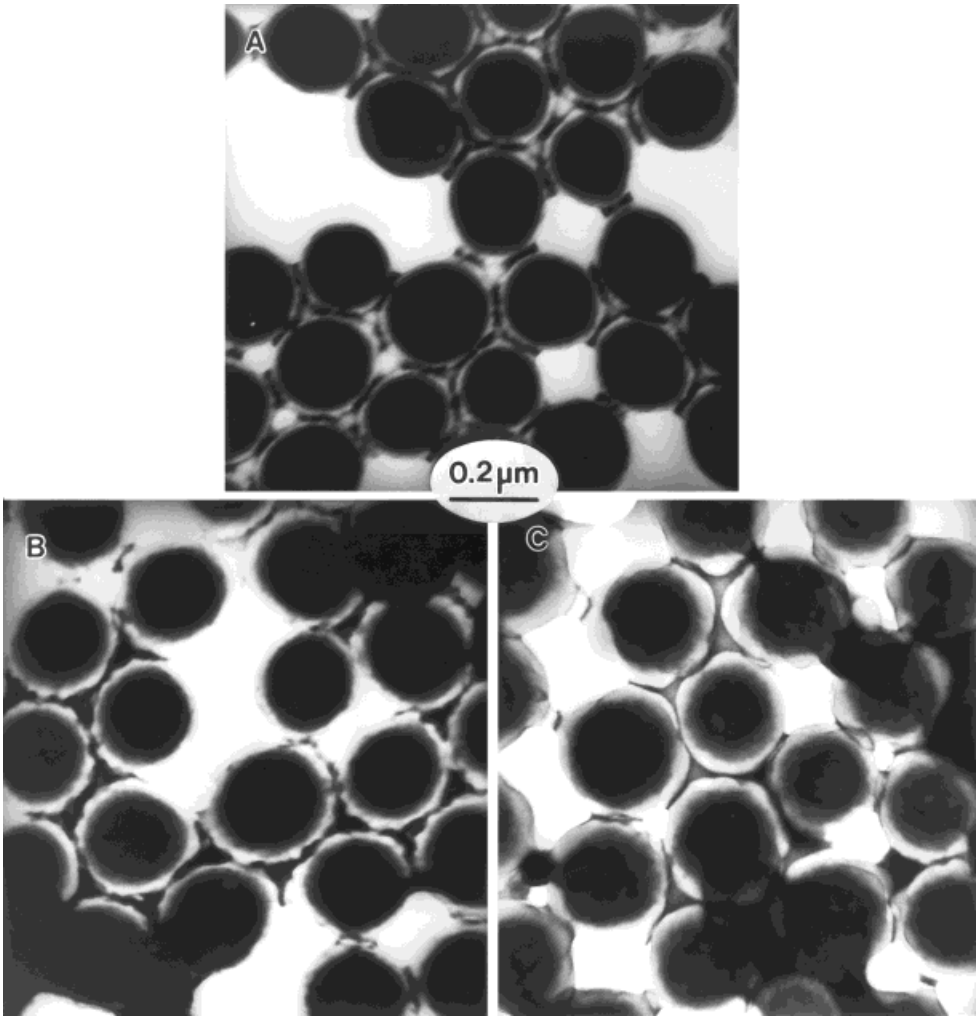

Figure 3 TEM micrographs of P(Bd/S)/SAN structured latexes prepared by semi-continuous emulsion polymerization: (A) C/S = 1/0.5; (B) C/S = 1/1; (C) C/S = 1/2. The shell copolymer composition (S/AN) = 72/28, KPS is 0.2 wt % based on the total recipe; P(Bd/S) cores used were of 180 nm-in diameter (by TEM) with 95% gel-fraction.

When this happens the observable shell layer became thinner. However, the core particles in all cases were still covered by a SAN shell polymer; the shell thickness increased with increasing the second stage monomer, which is similar to the case where the P(Bd/S) cores with 95% gel-fraction were used.

Measurement of the Degree of Grafting of SAN on P(Bd/S) core

The degree of grafting of the shell polymer on the core particles is an important factor in determining the toughness of the polymer matrix modified with structured latex particles. If the grafting is too low, the bonding between core and shell is not strong enough, and the core/shell particles can break easily in the core/shell interphase zone.

The effect of the initiator concentration and the monomer feed rate on the grafting efficiency of the shell polymer on the core particles was evaluated from the degree of grafting measurement. An increase in the KPS concentration from 0.06% to 0.2% resulted in about a 10% drop on the degree of grafting (from 82% to 69% based on shell polymer). It is well known that higher KPS concentrations generate more radicals, which increases the probability of termination reactions, forming free SAN, thus decreasing the probability of grafting. There is little effect for the duration of monomer feeding (3

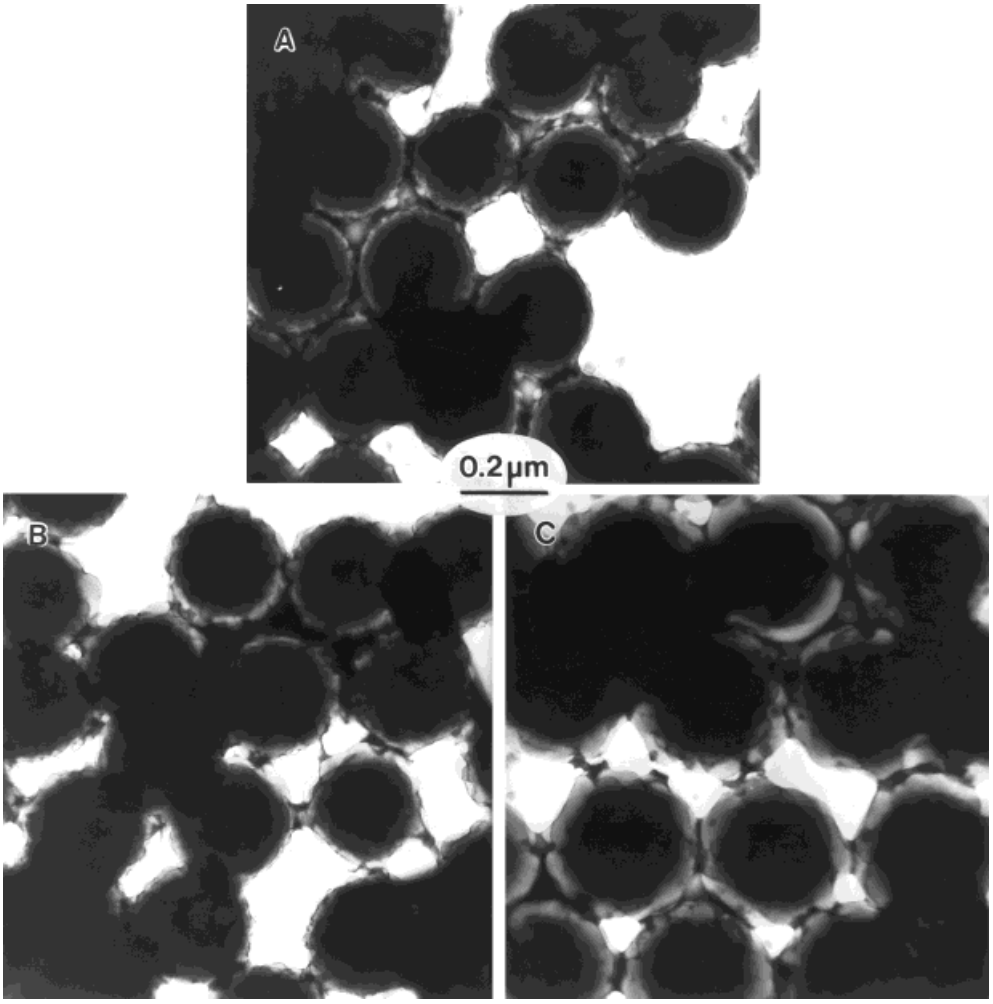

Figure 4 TEM micrographs of P(Bd/S)/SAN structured latexes prepared by semi-continuous emulsion polymerization: (A) C/S = 1/0.5; (B) C/S = 1/1; (C) C/S = 1/2. The shell copolymer composition (S/AN = 72/28). KPS is 0.2 wt % based on the total recipe. P(Bd/S) cores used were of 230 nm-in diameter (by TEM) with 40% gel fraction.

and 5 h) on the degree of grafting (compare 74% and 69% based on shell polymer).

The results for the effect of core/shell ratio and P(Bd/S) gel-fraction on the degree of grafting are given in Table V. Here, for both P(Bd/S) cores with 95% and 40% gel-fractions, the degree of grafting, expressed in terms of the percentage based on the total shell polymer, decreased with increasing shell content. The degree of grafting based on the unit weight of core, however, was increased with the increasing of the shell amount. This implies that the ability of the shell polymer to graft onto the P(Bd/S) core polymer is dependent on the concentration of the shell monomer. The higher the SAN concentration, the more SAN monomers are available to be grafted onto the P(Bd/S) cores, the grafted SAN molecular chains may be longer.

DSC Measurement

The glass transition temperatures (T_g) of P(Bd/S) cores, P(Bd/S)/SAN structured latex particles

Table V Effect of C/S Ratio and P(Bd/S) Gel Fraction on Degree of Grafting (D.G.) (KPS = 0.2%)

Gel-fraction %	Core/shell wt. ratio	D.G., % Based on Shell Polymer	D.G., g/g core
95	1/0.5	86	0.43
95	1/1	69	0.69
95	1/2	49	0.98
40	1/0.5	81	0.41
40	1/1	63	0.63
40	1/2	47	0.94

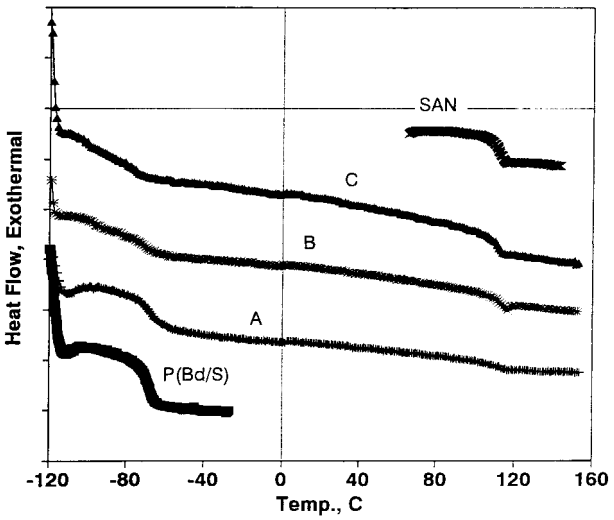

Figure 5 DSC results for P(Bd/S)/SAN structured latex particles: (A) C/S = 1/0.5; (B) C/S = 1/1; and (C) C/S = 1/2. P(Bd/S) with 95% gel fraction.

were determined from DSC. The T_g was taken as the temperature at which one-half of the change in heat capacity, ΔC_p, had occurred. Figure 5 is the results for P(Bd/S)/SAN polymers with different core/shell ratios, using 95% gel fraction P(Bd/S) cores. Two T_g are obtained for all the core/shell latex particles, corresponding to P(Bd/S) core and SAN shell, respectively. Same phenomena were observed for the core/shell latex particles using P(Bd/S) cores with 40% gel fraction. The T_g data are summarized in Table VI. The heat capacity, ΔC_p, changes with the different core/shell ratios: with increasing the shell amount, the ΔC_p decreased for the P(Bd/S) phase, while it increased for the SAN phase; which is proportional to the volume fraction of each phase.

DMS Measurement

Dynamic mechanical properties are the mechanical properties of materials as they are deformed under periodic (cyclic) forces. The dynamic modulus (E'), the loss modulus (E''), and a mechanical damping or internal friction express these properties. The dynamic storage modulus indicates the inherent stiffness of material under dynamic loading conditions. It may be shear, a tensile, or a flexural modulus, depending on the investigating technique. The mechanical damping or internal friction (E''/E', ratio of energy dissipated per cycle to the maximum potential energy stored during a cycle) indicates the amount of energy dissipated as heat during the deformation of the material, and is often expressed as tan δ. The dynamic loss modulus, or internal friction, is sensitive to many kinds of molecular motion, transitions, relaxation processes, structural heterogeneities, and the morphology of multiphase systems. Since the glass-rubber transition is the onset of motion of the molecular chains, the dynamic method provides a very direct determination of the transition temperature. The dynamic mechanical properties of polymers are usually studied over a wide temperature range. In the region where the dynamic modulus-temperature curve has an inflection point, the internal friction (tan δ) curve goes through a maximum. This point is called the glass-transition region where the dynamic storage modulus changes from the glassy state (10^9 Pa) to the soft rubbery state (10^6 Pa). The E'' goes through a peak at slightly lower temperature than tan δ. The maximum heat dissipation per unit deformation occurs at the temperature where E'' is maximum.

Figures 6 and 7 show the dynamic storage shear modulus (G') and loss shear modulus (G'') versus temperature and tan δ versus temperature curves for the P(Bd/S)/SAN structured latex particles using P(Bd/S) cores with 95% gel fraction, respectively. Similar results were obtained for the P(Bd/S)/SAN latex particles using P(Bd/S) cores with 40% gel-fraction. The T_g values shown

Table VI Glass Transition Temperatures from DSC Measurement

Polymer	T_g, °C	ΔC_p, J/gK
P(Bd/S) core with 95% G.F.	− 68	0.48
1/0.5 P(Bd/S)/SAN	− 67, 111	0.282, 0.054
1/1 P(Bd/S)/SAN	− 68, 112	0.11, 0.075
1/2 P(Bd/S)/SAN	− 73, 112	0.084, 0.191
P(Bd/S) core with 40% G.F.	− 70	0.573
1/0.5 P(Bd/S)/SAN	− 67, 112	0.265, 0.042
1/1 P(Bd/S)/SAN	− 67, 111	0.122, 0.077
1/2 P(Bd/S)/SAN	− 70, 112	0.115, 0.143
SAN	113	0.369

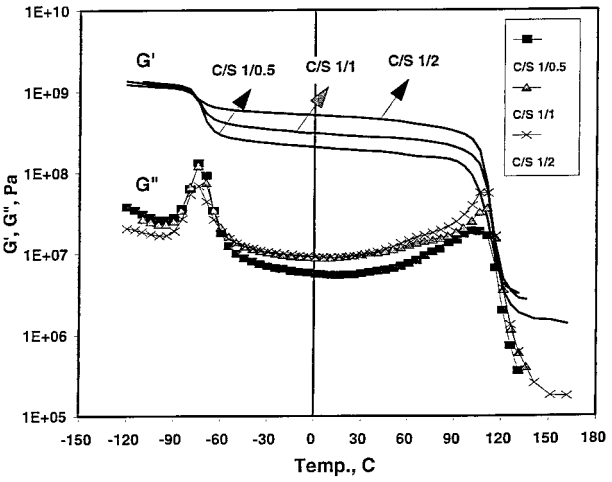

Figure 6 G' and G'' versus temperature curves for P(Bd/S)/SAN structured latex particles with different C/S ratios; P(Bd/S) particles with 95% gel fraction.

in Table VII are determined from the loss shear modulus and tan δ peaks.

It can be seen that the T_g values from G'' peaks for most samples are $\sim$ 5°C lower than from tan δ peaks. Most importantly, all the core/shell samples show two T_g, corresponding to the P(Bd/S) core and SAN shell glass transitions, respectively. In addition, since the shell polymer, SAN, has higher storage modulus at the glassy state, the magnitude of the storage shear modulus G', changing from glassy state to rubbery state reasonably decreases with decreasing the core/shell ratio from 1/0.5 to 1/2.

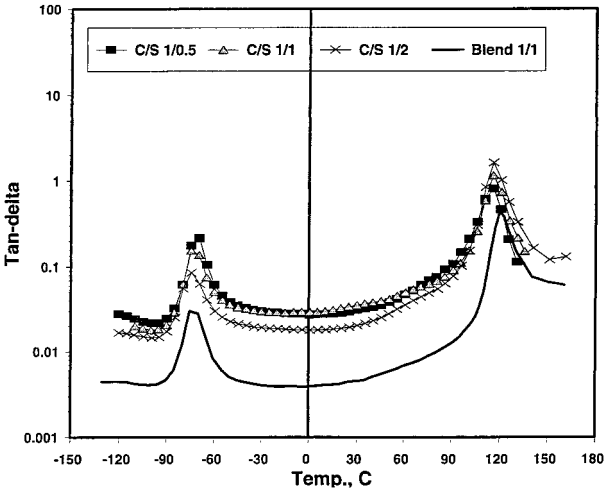

Figure 7 Tan-delta versus temperature curves for P(Bd/S)/SAN structured latex particles with different C/S ratios; P(Bd/S) particles with 95% gel fraction.

Table VII Glass Transition Temperatures From DMS Measurement

	T_g, °C	
Polymer	from G'' peak	from tan δ peak
P(Bd/S) core with 95% G.F.	−75	−70
1/0.5 P(Bd/S)/SAN	− 74, 101	− 69, 116
1/1 P(Bd/S)/SAN	− 74, 111	− 69, 116
1/2 P(Bd/S)/SAN	− 74, 109	− 74, 116
P(Bd/S) core with 40% G.F.	− 75	− 75
1/0.5 P(Bd/S)/SAN	− 75, 101	− 70, 116
1/1 P(Bd/S)/SAN	− 75, 111	− 70, 116
1/2 P(Bd/S)/SAN	− 74, 111	− 69, 116
SAN	111	121

From Figure 6, it is also shown that there is a small peak around 60°C. It is very possibly due to the grafting of SAN polymer on P(Bd/S) cores, forming a copolymer of SAN and P(Bd/S). From the measurement of degree of grafting of SAN polymer on the P(Bd/S) core polymers (Table VI), 41–87% SAN based on the total shell amount were grafted, which confirms these peaks $\sim$ 60°C are caused by the grafting of SAN polymer on the core polymers. But from the tan δ versus temperature plot (Fig. 7), the curves does not show much difference from that of the blend of P(Bd/S) core and SAN shell polymers. From the T_g values in both Tables VI and VII, they suggest little mixing of the core and shell components. This implies that even though some SAN is polymer grafted on the core polymers, most of SAN polymer still forms its domains, showing its T_g.

CONCLUSIONS

Monodisperse P(Bd/S) (90/10 by wt) latex particles with different particle sizes (180–520 nm from light scattering measurement) were prepared by conventional emulsion polymerization. By controlling the conversion and the emulsifier concentration, similar particle sizes P(Bd/S) with 95 and 40% gel fractions were obtained, which were used as the cores for the preparation of structured latex particles.

By semicontinuous emulsion polymerization, P(Bd/S) core/SAN shell type morphology particles were synthesized. Increasing the initiator concentration favored the uniform shell forma-

tion. The particle morphologies for the core/shell particles with different gel fractions are similar. The shell thickness was controlled by verifying the core polymer/shell monomer weight ratio. However, when using P(Bd/S) with 40% gel fraction, the shell was thinner and not as smooth as when using P(Bd/S) with 95% gel fraction. The degree of grafting for the SAN onto P(Bd/S) cores was affected by the initiator concentration; the higher the initiator concentration, the lower the degree of grafting as a result of lower SAN molecular weights.

The T_g of P(Bd/S) core and P(Bd/S)/SAN structured latex particles was characterized both by DSC and DMS. Two T_g were observed for the core/shell structured latex particles, for the P(Bd/S) and SAN, respectively. The intensity of the transition peak changes proportionally with change of the core/shell ratio, as expected theoretically. The crosslinking density of the P(Bd/S) core has little effect on the glass transitions of the core and shell polymers.

REFERENCES

1. L. W. Morgan, *J. Appl. Polym. Sci.,* **27,** 2033 (1982).
2. D. I. Lee and T. Ishikawa, *J. Polym. Sci., Polym. Chem. Ed.,* **21,** 147 (1983).
3. I. Cho and K. W. Lee, *J. Appl. Polym. Sci.,* **30,** 1903 (1985).
4. M. Okubo, *Makromol. Chem., Macromol. Symp.,* **35/36,** 307 (1990).
5. J. Berg, D. Sundberg, and B. Kronberg, *Polym. Mater. Sci. Eng.,* **54,** 367 (1986).
6. Y. Cheng, V. L. Dimonie, and M. S. El-Aasser, *J. Appl. Polym., Sci.,* **42,** 1049 (1991).
7. S. Lee and Rudin, in *Polymer Latexes,* E. Daniels, E. D. Sudol, and M. S. El-Aasser, Eds., ACS Symposium Series, **492,** 234 (1992).
8. G. A. Vandezande and A. Rudin, *J. Coatings Tech.,* **66,** 99 (1994).
9. D. G. Cook, A. Rudin, and A. Plumtree, *J. Appl. Polym. Sci.,* **46,** 1387 (1992).
10. D. G. Cook, A. Rudin, and A. Plumtree, *J. Appl. Polym. Sci.,* **48,** 75 (1993).
11. D. W. Gilmore and M. J. Modic, *Plastics Eng.,* **April,** 51 (1989).
12. J. I. Eguiazabal and J. Nazabal, *Polym. Eng. & Sci.,* **30,** 527 (1990).
13. J. Y. Qian, R. A. Pearson, V. L. Dimonie, and M. S. El-Aasser, *J. Appl. Polym. Sci.,* **58,** 439 (1995).
14. D. S. Parker, H-J Sue, J. Huang, and A. F. Yee, *Polymer,* **31,** 2267 (1990).
15. F. C. Chang, J. S. Wu, and L. H. Chu, *J. Appl. Polym. Sci.,* **44,** 491 (1992).
16. C. Cheng, A. Hiltner, E. Baer, P. R. Soskey, and S. G. Mylonakis, *J. Appl. Polym. Sci.,* **52,** 177 (1994).
17. C. Cheng, N. Peduto, A. Hiltner, E. Baer, P. R. Soskey, and S. G. Mylonakis, *J. Appl. Polym. Sci.,* **53,** 513 (1994).
18. B. S. Lombardo, H. Keskkula, and D. R. Paul, *J. Appl. Polym. Sci.,* **54,** 1697 (1994).
19. I. Segall, V. L. Dimonie, M. S. El-Aasser, P. R. Soskey, and S. G. Mylonakis, *J. Appl. Polym. Sci.,* **58,** 385 (1995).
20. I. Segall, V. L. Dimonie, M. S. El-Aasser, P. R. Soskey, and S. G. Mylonakis, *J. Appl. Polym. Sci.,* **58,** 401 (1995).
21. I. Segall, V. L. Dimonie, M. S. El-Aasser, P. R. Soskey, and S. G. Mylonakis, *J. Appl. Polym. Sci.,* **58,** 419 (1995).
22. T. A. Callaghar, K. Takakuwa, D. R. Paul, and A. R. Padwa, *Polymer,* **34,** 3796 (1993).
23. J. Im, A. Hiltner, and E. Baer, in *High Performance Polymers,* E. Baer and A. Moet, Eds., Hanser, New York, 175 (1991).
24. J. D. Keitz, J. W. Barlow, and D. R. Paul, *J. Appl. Polym. Sci.,* **29,** 3131 (1984).
25. V. Tanrattanakul, E. Baer, A. Hiltner, R. Hu, V. L. Dimonie, M. S. El-Aasser, L. H. Sperling, and S. G. Mylonakis, *J. Appl. Polym. Sci.* **62,** 2005 (1996).
26. T. T. Serafini and E. G. Bobalek, *Official Digest,* October, 1259 (1960).
27. L. H. Sperling, *Introduction To Physical Polymer Science,* Wiley, New York, (1992), chapter 7, appendix 7.3.
28. G. Odian, in *Principles of Polymerization,* 2nd ed., Wiley, New York, 331 (1981).